Zhang, Jia et al.

Article

Enhanced performance of photovoltaic-thermoelectric coupling devices with thermal interface materials

Energy Reports

Provided in Cooperation with:
Elsevier

Suggested Citation: Zhang, Jia et al. (2020) : Enhanced performance of photovoltaic-thermoelectric coupling devices with thermal interface materials, Energy Reports, ISSN 2352-4847, Elsevier, Amsterdam, Vol. 6, pp. 116-122, https://doi.org/10.1016/j.egyr.2019.12.001

This Version is available at:
https://hdl.handle.net/10419/244018

Energy Reports 6 (2020) 116–122

Contents lists available at ScienceDirect

Energy Reports

journal homepage: www.elsevier.com/locate/egyr

Research paper

Enhanced performance of photovoltaic–thermoelectric coupling devices with thermal interface materials

Jia Zhang [a], Han Zhai [b], Zihua Wu [a,*], Yuanyuan Wang [a], Huaqing Xie [a,b], Mengjun Zhang [a]

[a] School of Environmental and Materials Engineering, Shanghai Polytechnic University, Shanghai 201209, China
[b] School of Energy and Power Engineering, Nanjing University of Science and Technology, Nanjing 210009, China

ARTICLE INFO

Article history:
Received 23 August 2019
Received in revised form 22 November 2019
Accepted 3 December 2019
Available online xxxx

Keywords:
PV–TE coupling device
Thermal interface material
Thermal contact resistance
Output power

ABSTRACT

In this study, thermal interface material is used in photovoltaic–thermoelectric coupling device to enhance the utilization of solar energy. An operating system including cooling equipment is established. The output performance evolutions of PV–TE coupling device are carried out based on thermal contact resistance under different experimental conditions. The PV–TE coupling devices combine with monocrystalline silicon PV cell and bismuth telluride TEG. Results show that adding TEG could minimize the PV cell temperature increase, hence improving PV cell performance effectively. Results also indicate that, with thermal interface material, the power generation by PV cells increases at least 14% and the power generation by TEG increases at least 60% due to the decreasing thermal contact resistance. Applying thermal interface material enhances the heat transfer in PV–TE coupling device.

1. Introduction

Photovoltaic (PV) cell, which directly convert solar energy into electricity based on the principle of photoelectric conversion, has been widely used for their advantages such as pollution-free, and long-term energy demand (Tyagi et al., 2013; Wysocki and Rappaport, 1960). However, PV cell is weak in utilizing the full spectrum of solar radiation in the accordance with Shockley–Queisser limit. PV cells can harvest part of the ultraviolet (UV) and visible light of the solar spectrum into electricity, most of the infrared radiation (IR) energy is stored in the cell as heat (Thirugnanasambandam et al., 2010). Cooling PV cells is a major requirement due to the temperature growth may lead PV cell experience the performance loss (Radziemska, 2003; Skoplaki and Palyvos, 2009). Thermoelectric generator (TEG) can convert heat directly into electric energy induced by the Seebeck effect when the temperature difference exists (TrittT et al., 2008; He et al., 2015; Liu et al., 2014; Venkatasubramanian et al., 2001; Zhang et al., 2015). In recent years, photovoltaic–thermoelectric (PV–TE) coupling system has attracted much attention to enable full spectrum of solar radiation can be utilized by PV cells. One of the widely applied coupling methods is to paste the TEG on the back of the PV cell (Huen and Daoud, 2016). Meneses-RodríGuez et al. (2005) proposed that PV–TE system the total efficiency can reach 20%–25% when the cold side temperature of the TEG module maintained at 30 °C. Vorobiev et al. (2006) designed two types of coupling system including directly coupling and spectrum splitting coupling. The simulation results showed that both hybrid systems are efficient and practical. Deng et al. (2013) investigated the bowl-shaped PV–TE coupling system. They indicated that the coupling system could generate as much as twice output power in comparisons of the pure PV cell. Liao et al. (2014) proposed theoretically a low concentrating PV–TE coupling model where connected the load resistance connection in the external circuit and addressed the optimized parameters. These works proved that PV–TE coupling system is a constructive proposal. There are several factors affect the performance of the PV–TE coupling system. Two of the most important factors are the cooling condition (Zhang et al., 2014; Pang et al., 2015; Wu et al., 2015; Yin et al., 2017) and thermal contact resistance (TCR) (Qiu et al., 2017; Chen and Xuan, 2015; Grujicic et al., 2005). Zhang et al. (2014) studied a concentrated PV–TE coupling system with forced air cooling theoretically and found the system efficiency increased by 30% compared with the pure PV cell. Pang et al. (2015) applied pin-fin heat sink in the PV–TE coupling system and found that the PV–TE system was cooled by about 30 °C, which enhanced the total efficiency the PV–TE system up to 5.9%. Wu et al. (2015) applied the nanofluid as the cooling medium theoretically and found the output power of the PV–TE coupling system was increased effectively. In the work of Yin et al. (2017), different types of cooling method were compared, including the water cooling, the natural cooling and the air forced cooling. Results showed that water cooling was the most effective cooling

* Corresponding author.
E-mail address: wuzihua@sspu.edu.cn (Z. Wu).

https://doi.org/10.1016/j.egyr.2019.12.001

method. In addition, the conduction of waste heat generated by PV cells to the TEG inevitably passed through the interfaces, resulting in thermal contact resistance (TCR), which has crucial impact on the performance of PV–TE coupling system (Zhang et al., 2014; Yin et al., 2017; Qiu et al., 2017; Chen and Xuan, 2015; Grujicic et al., 2005). Zhang et al. (2014) found the total efficiency of the coupling system can be higher or lower than pure-PV system, depends on the TCR. Yin et al. (2017) proved that the efficiency of the PV–TE coupling system would be even lower than that of the pure PV cell if the TCR between PV and TEG does not match the figure of merit (ZT value) of the thermoelectric material. Qiu et al. (2017) made a quantitative comparison between the contribution of thermal conductivity of carbon nanotube array and thermal contact resistance at carbon nanotube array-solid interface to heat transfer. They found that the total thermal resistance is mainly attributed to the TCR at the interface. Chen and Xuan (2015) explored the effect of TCR caused by roughness interface on heat transfer theoretically and declared that heat transfer would decreased by a very small TCR. Grujicic et al. (2005) pointed out that the TCR could be reduced by thermal interface material (TIM). Mirmira et al. (1997) investigated the influence of TIM on the contact surface experimentally and found that the thermal conductivity was the vital factor. But their experimental results are not conducted in PV–TE coupling system (Qiu et al., 2017; Chen and Xuan, 2015; Grujicic et al., 2005; Mirmira et al., 1997). Based on the literatures addressed above, it has been widely accepted that the TCR has obvious influence on the performance of PV–TE coupling system and TIM such as thermal grease, phase change materials and so on could be applied to tune the TCR (Prasher, 2001). However, the heat transfer mechanisms at the interface between the PV cell and the TEG module need further study. The optimized performance of TIM with different conductivity on the coupling devices should also be evaluated. Therefore, in this work, we will study the heat transfer situation between PV cell and TEG with different cooling conditions, solar irradiation and TIM applied, by establishing a PV–TE coupling device with two external electrical circuits connecting load resistances respectively. The rest of this manuscript is organized as follows. In Section 2, the experimental setup and the measurement methods are presented. Then in Section 3 the performance of the PV–TE coupling devices are explored. Firstly, the performance of pure PV cell and the PV–TE directly coupling device are studied. Secondly, the effects of TIM on the PV–TE coupling devices are studied. Finally, this work is concluded in Section 4.

2. Experimental methods

Fig. 1(a)(b) shows the structure and photograph of the PV–TE coupling device, which consists of a mono-crystalline silicon PV cell, a TIM coating layer and a bismuth telluride TEG module. PV cell and TEG module are purchased from Ningbo Sibranch International Trading Co., Ltd. and Hangzhou Dahe Thermo-Magnetics Co., Ltd. respectively. Their parameters are shown in Table 1. The back of PV cell is uniformly coated with TIM. The TIM used in this experiment is the thermal grease which have the advantages of high thermal conductivity, no delamination, no curing required, and low thermal resistance (Sarvar et al., 2006; Qiu et al., 2018). Then the PV cell and TEG are packaged into a coupling device with Ethylene Vinyl Acetate Copolymer (EVA) to protect the PV cell. As Fig. 1(c) illustrated, in PV–TE coupling device, when PV cell exposed to radiation confront with sunlight, the electrons will be promoted from the valence band to conduction band, leaving electron holes when the absorbed energy is equal to or greater than the bandgap energy. Electrons flow in the external circuit, and thus generating current. Energy that cannot be used by PV cell is converted into heat and then conducts to TEG. TEG is made of numbers of thermoelectric couples which are consisted of p-type (hole carriers) and n-type (electron carriers) semiconductor materials. The temperature difference results in higher density of hole and electron at the hot side because of the strong thermal excitation. Driven by this carrier density gradient, holes and electrons diffuse to and finally recombine at the cold side of TEG low. This process creates a potential difference and drives a current flow in the external circuit (Ma et al., 2015). Fig. 1(d)(e) gives the photo of the experimental and measuring instruments. Under the PV–TE coupling device, a thermostatic cooling system is applied, including a copper heat sink, a thermostatic bath, and a peristaltic pump. The heat sink and the bottom of the coupling device are coated with thermal grease with 4.2 W m^{-1} K^{-1} to isolate air. The coupling devices are tested under a simulative sunlight (Ceaulight Co., Ltd). The experimental irradiance of the simulator is measured by a pyranometer (Ophir NOVA II). PV cell and TEG are connected with standard resistances R_{PV-S} and R_{TE-S} in series respectively purchased from Shanghai Chengyang Instrument and Meter Co., Ltd. The loading resistances of PV cell circuit and TEG circuit including series resistance and internal resistance of the lead wires are R_{PV-L} and R_{TE-L} respectively. Voltmeters (Keithley 2002 Multimeter) are used to measure the distributed voltages of the loading resistances during the stable states of the PV cell and the TEG. In order to obtain the value of the temperature with higher accuracy, Aglient 34970A data-logger installed with a 20-channel multiplexor is used.

Table 1
Parameters of the PV cell and the TEG module.

Components	Parameters	Value
PV cell (25 °C, 1000 W/m^2)	Size (mm × mm)	37.5 × 37.5
	Height (mm)	0.3
	Photoelectric conversion efficiency (%)	20
	Open circuit Voltage (V)	0.645
	Short circuit Current (A)	9.446
	Fill Factor (%)	80.36
TEG (25 °C, 1000 W/m^2)	Material type	Bi_2Te_3
	Hot side size (mm × mm)	40 × 40
	Cold side size (mm × mm)	40 × 40
	Height (mm)	3.35
	Number of $p-n$ pairs	199

A T-type thermocouple is arranged on the upper surface of the EVA to obtain the upper surface temperature T_1, which is approximated to be the temperature of the PV cell since the outer EVA sealant is very thin. Another two K-type thermocouples are also applied, one of which is placed inside a hole drilled at the central position of the top of the heat sink to measure the temperature of the cold side which is labeled as T_2, and the other one of which is placed on the experimental table to measure the ambient temperature. All the measurement error of the thermocouples applied is 0.1 °C. We study four types of experimental samples including the pure PV cell, the direct contact PV–TE coupling device, the PV–TE coupling device with thermal grease 1, the PV–TE coupling device with thermal grease 2, which is labeled as S_p, S_0, S_1, and S_2, respectively. Firstly, to investigate the effect of adding TEG on PV cell, we measure the temperature of PV cell in the pure system (S_p) and the direct contact PV–TE coupling device (S_0) in the same condition. These two temperatures of upper PV cell are labeled as T_1^{PV} and T_1^{PV-TE}, respectively. Then we introduce the temperature difference of these two temperatures to evaluate the effect of the TEG module on the performance of the PV system, which is expressed as $\Delta T_1 = T_1^{PV} - T_1^{PV-TE}$.

The output powers distributed by the loading resistance in the pure PV cell and the PV–TE coupling device are measured.

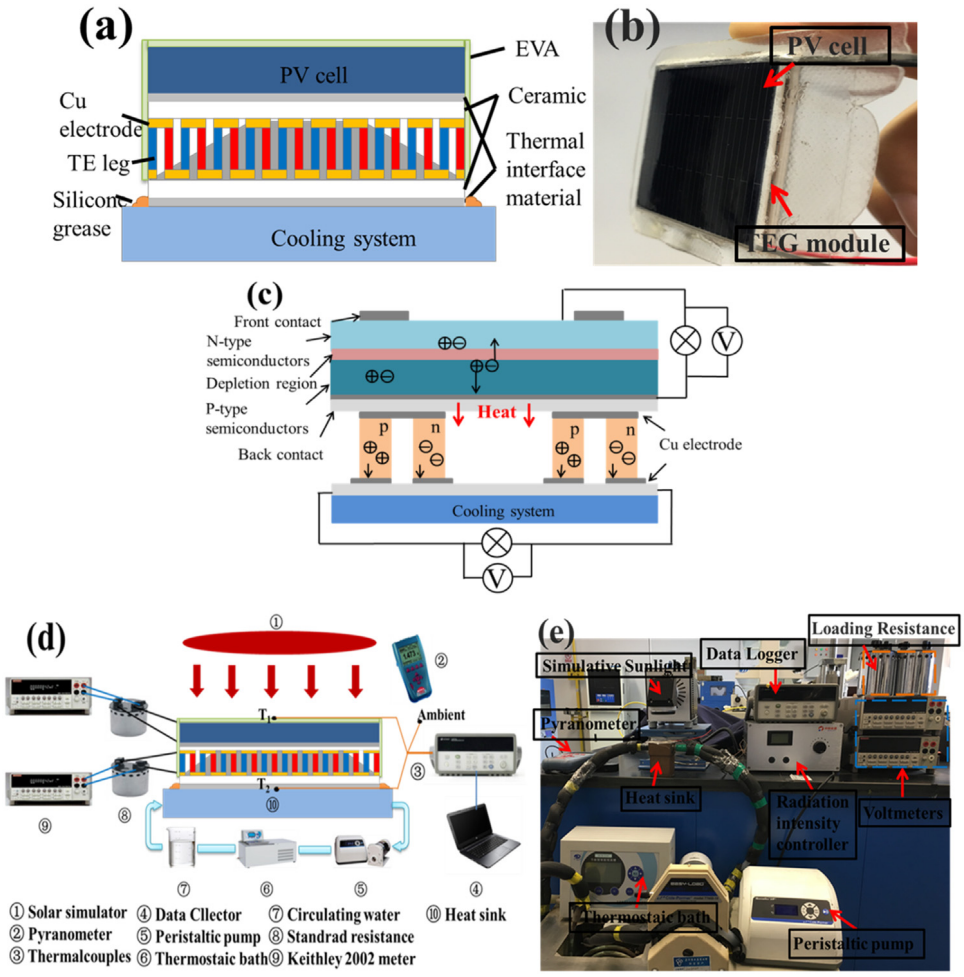

Fig. 1. (a) Structure of the PV–TE coupling device (b) Photograph of the PV–TE coupling device. (c) Carrier transfer process of PV–TE coupling devices under illumination and thermal gradient (d) Schematic diagram of the experimental and measuring instruments (e) Photo of the experimental and measuring instruments.

Next, directly contact coupling device (S_0) and the PV–TE coupling device with thermal grease 1 (S_1), the PV–TE coupling device with thermal grease 2 (S_2) in different conditions are compared to investigate the influence of thermal contact resistance on PV–TE coupling device performance. The thermal conductivity of thermal grease 1 is 1.0 W m^{-1} K^{-1}, and the one of thermal grease 2 is 4.2 W m^{-1} K^{-1}.

Two types of radiation intensities, 250 mW/cm^2 and 350 mW/cm^2, are applied. Four types of cooling conditions are applied, including the natural cooling, the water cooling temperature being 25 °C, 20 °C, and 15 °C. It should be noticed that the tested samples are not connected to the cooling system when natural cooling is applied.

Considering the influence of wire internal resistance and contact resistance, neglecting the wire internal resistance may result in a large error in calculating the output power. So we calculate the internal resistance of the wires into the total loading resistance. The series resistances in PV cell circuit (R_{PV-S}) and TEG circuit (R_{TE-S}) are all 1.0 Ω. The total loading resistance in PV cell circuit (R_{PV-L}) and TEG circuit (R_{TE-L}) are 2.6 Ω and 2.0 Ω, respectively. After measuring the voltage of PV cell (U_{PV}) and the voltage of TEG (U_{TE}), the output power of PV cell (P_{PV}) and that of the TEG (P_{TE}) are calculated by:

$$P_{PV} = \left(\frac{U_{PV}}{R_{PV-S}}\right)^2 R_{PV-L} \quad (1)$$

$$P_{TE} = \left(\frac{U_{TE}}{R_{TE-S}}\right)^2 R_{TE-L} \quad (2)$$

The total output power of the PV–TE coupling device P can be obtained as follows:

$$P = P_{PV} + P_{TE} \quad (3)$$

In the measurement, all the data of temperature and voltage are obtained under steady-state and recorded every one second. Then forty times of records are collected and average to get the final data. In addition, all the experiments are carried out under natural convection conditions. The vertical error bars represent the standard deviation from repeated measurements date across figures at different experimental condition.

3. Results and discussion

3.1. The effect of coupling TEG module on PV cell

In this subsection, the temperature characteristic of the PV cell and the output power are compared between the pure PV cell and the PV–TE coupling device. Fig. 2(a) shows the properties of the upper surface temperature T_1 of the pure PV cell (S_p) and the direct contact PV–TE coupling device (S_0) in different cooling and radiation conditions. It can be found that T_1 of the coupling device (S_0) is always lower than that of the pure PV cell (S_p), which implies that adding TEG module can suppress the temperature increase of PV cell effectively. Then we pay attention on the temperature difference of PV cell (ΔT_1) between the pure PV cell and the PV–TE coupling devices, which is shown

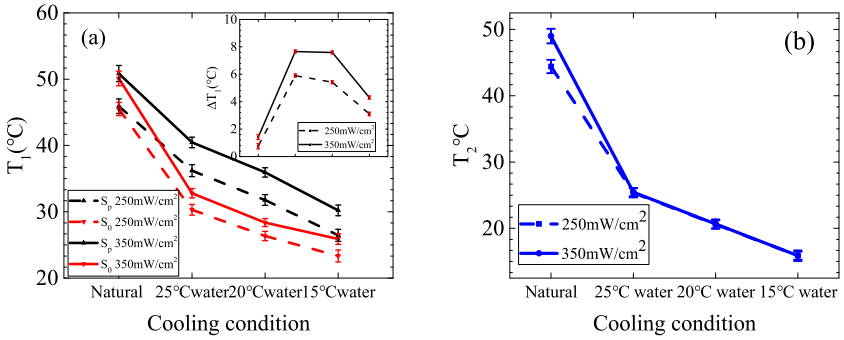

Fig. 2. (a) The temperatures of the PV cell (T_1), (b) the cold side of the TEG module (T_2) and vary with the cooling and radiation conditions. Insert: temperature difference between the pure PV cell and PV–TE coupling devices (ΔT_1) varies with the cooling and radiation conditions. Therein, the solid curves represent exposure to G_1 radiation, the dashed curves represent exposure to G_2 radiation.

in the insert of Fig. 2(a). The highest temperature difference of PV cell (ΔT_1) is about 7.65 °C when 25 °C water cooling and 350 mW/cm^2 is applied. Then we notice that the temperature difference ΔT_1 decreases with the decrease of the cooling temperature. This is mainly because the temperature dependence of PV cell performance. The effect of coupling TEG on suppressing PV cell temperature rise is more remarkable at higher temperature. PV cell which benefits from excellent heat dissipation will keep better performance. When natural cooling is used, the temperature difference ΔT_1 is smallest (∼0.75 °C). It indicates that TEG has little effect on the PV device in poorly cooling condition. The temperature differences all decrease when the radiation is decreased, which implies that TEG has more obvious effect on the PV–TE coupling device when stronger radiation is applied. Fig. 2(b) shows properties of the temperatures of the cold side of TEG (T_2) in different cooling and radiation conditions. The results imply that the water cooling achieves better refrigeration effect in comparison with the natural cooling. The designed cooling system plays an important role as external heat exchanger, achieving instantaneously heat dissipation (Baranowski et al., 2013). In the experiment process, the ambient temperature almost keeps unchanging, which indicates that our results shown above are not affected by environment.

The output powers of the pure PV cell (S_p) and the direct contact PV–TE coupling device (S_0) is compared to investigate the effect of introducing TEG. Fig. 3(a) shows that the output power of PV cell (P_{PV}) of the directly contact PV–TE coupling device (S_0) is always higher than that of the pure PV cell (S_p), no matter which cooling and radiation condition is applied. This result implies that the coupling of PV cell and TEG could improve the performance of PV cell effectively. Fig. 3(a) shows, with water cooling condition, P_{PV} of S_0 is much higher than S_p. For example, the output power of the PV cell (P_{PV}) of S_0 is about 3.84% higher than S_p when the 25 °C water cooling and 350 mW/cm^2 radiation is applied. In contrast, the corresponding increase is only 2.62% when the natural cooling condition and 350 mW/cm^2 radiation is applied. The increases of P_{PV} in the directly contact PV–TE coupling (S_0) device remains almost the same with different radiation condition applied. Fig. 3(b) shows the output power of TEG (P_{TE}) of directly contact PV–TE coupling device (S_0). TEG can reuse the heat generated by PV cells additionally barely with cooling effect. The output power of TEG (P_{TE}) is 1.21 mW when 15 °C water cooling and 350 mW/cm^2 radiation is applied. And P_{TE} is less than 0.01 mW with natural cooling applied no matter which radiation is applied. Fig. 3(c) shows the total output power (P) of pure PV cell (S_p) and PV–TE directly contact coupling device (S_0). The total output power (P) of the PV–TE coupling device (S_0) is always higher than that of the pure PV cell (S_p). The total output power (P) increases by 4.65% when the 20 °C water cooling and 350 mW/cm^2 radiation is applied. Coupling PV cell with TEG could indeed suppress the temperature rise of PV cell and improve the P_{TE}. The disadvantage of PV cell can be compensated by utilized the advantage of TEG module cause PV cell and TEG module two devices have complimentary characteristics. Not only can TEG module makes dual function of cooling PV cell also producing additional energy. Cooling condition is also an important factor affecting the performance of PV cell and TEG. Instantaneous refrigeration effect could improve the P_{PV} and minimize the negative influence of temperature on PV cells. If it can be properly cooled and the sufficient temperature difference across it, TEG can utilize the more unwanted heat to generate electrical energy. What should note is that the output power of PV cell (P_{PV}) improves slightly. P_{TE} is minuteness correspondingly, not obtaining expected.

3.2. The effect of thermal interface materials on PV–TE coupling devices

In this subsection, we attempt fabricating the PV–TE coupling device that coating two types thermal grease on the back of PV cells to investigate its effect on ameliorating thermal contact resistance. Fig. 4(a) shows the output power of PV cells (P_{PV}) of the PV–TE coupling device varies with the thermal greases coated under 250 mW/cm^2 radiation. P_{PV} increases obviously with the increase of thermal conductivity. The largest increases of P_{PV} between the case without thermal grease (S_0) and that with 4.2 W m^{-1} K^{-1} thermal grease PV–TE coupling device (S_2) reaches 22.5% when 250 mW/cm^2 radiation and 15 °C water cooling condition is applied. This result indicates that coating TIM can reduce TCR and enhance the heat transfer from PV cells to TEGs, which is beneficial to the heat dissipation of PV cells and thus improves the output power of PV cells observably. Fig. 4(b) shows the corresponding results with larger radiation (350 mW/cm^2) applied. The output power of PV cells (P_{PV}) of the coupling devices increases with the radiation enhances. When 25 °C water cooling is applied, P_{PV} of PV–TE coupling device with 4.2 W m^{-1} K^{-1} thermal grease (S_2) increases by 8.9% as the radiation enhances. This result mainly because the photoelectric characteristics of PV cell. More electrons excited to the conduction band when illuminated with stronger radiation, and the carrier concentration increases. More electrons flow to the external circuit leading the enhancing electrical output of PV cell (Dubey et al., 2013).

The properties of the output power of TEGs (P_{TE}) of the PV–TE coupling devices that varies with the thermal greases coated are shown in Fig. 5. Fig. 5(a) shows that P_{TE} of the PV–TE coupling devices is greatly improved by adopting the thermal greases. The maximum increase of P_{TE} is about 102.86% for the case with coating 4.2 W m^{-1} K^{-1} thermal grease (S_2) when the 15 °C water cooling is applied. Result indicates that the heat drop

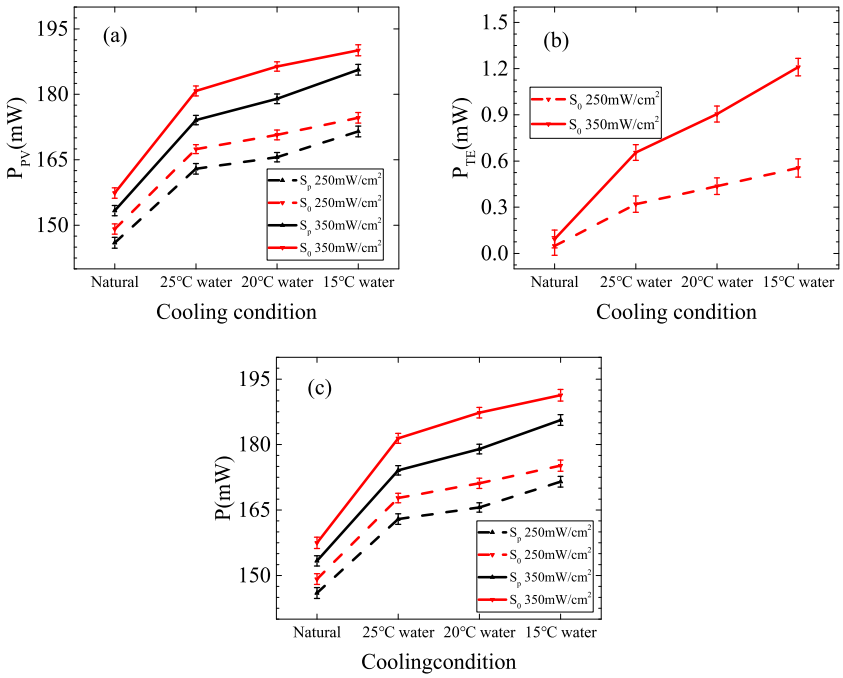

Fig. 3. The output powers of (a) PV cells (P_{PV}), pure PV cell (S_p) and PV–TE directly coupling device (S_0), (b) TEG (P_{TE}), PV–TE directly coupling device (S_0), (c) total output power (P) of pure PV cell (S_p) and PV–TE directly coupling device (S_0) vary with the cooling and radiation conditions. Therein, the solid curves represent exposure to 250 mW/cm^2 radiation and the dashed curves represent exposure to 350 mW/cm^2 radiation.

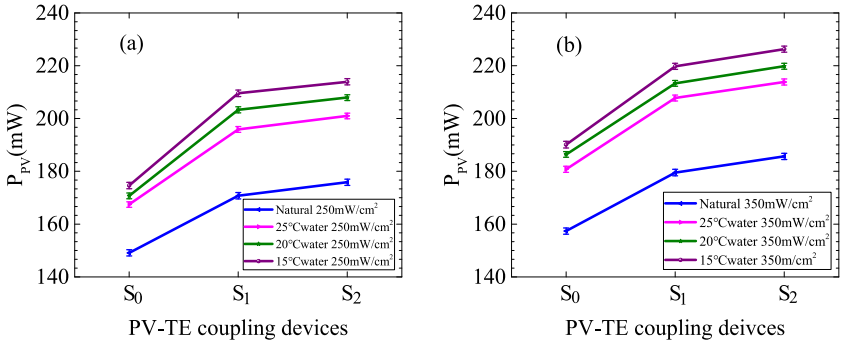

Fig. 4. The output power of PV cells (P_{PV}) of the PV–TE coupling devices vary with the thermal greases with (a) G_1 and (b) G_2 radiation and different types of cooling conditions applied.

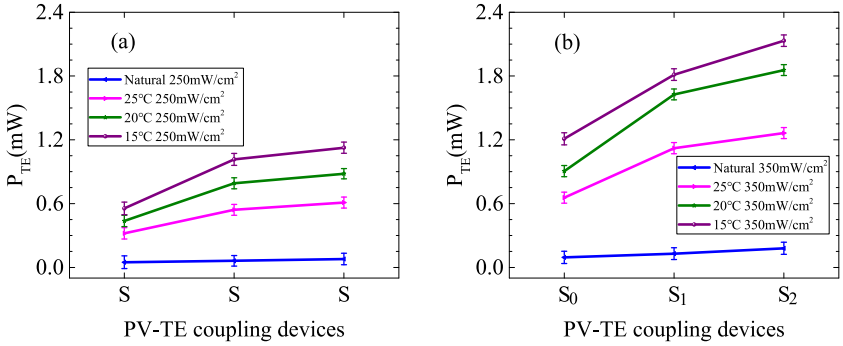

Fig. 5. The output powers of TEG (P_{TE}) of the PV–TE coupling devices vary with the thermal greases with (a) 250 mW/cm^2 and (b) 350 mW/cm^2 radiation and different types of cooling conditions applied.

during the transfer process can be obviously decreased with the utilization of thermal grease. Meanwhile, cooling condition can affect P_{TE} strongly. Compared with natural cooling, the output power of TEGs (P_{TE}) of the PV–TE coupling device with 4.2 W m^{-1} K^{-1} thermal grease (S_2) coating applied is increased by 14.36 times when 15 °C water cooling is used. The performance of TEGs presents a tendency with logarithmic increasing when using water cooling. Fig. 5(b) shows the corresponding results when the radiation enhances. TEGs have the analogous performances with PV cells because enhancing radiation makes TEGs absorbing

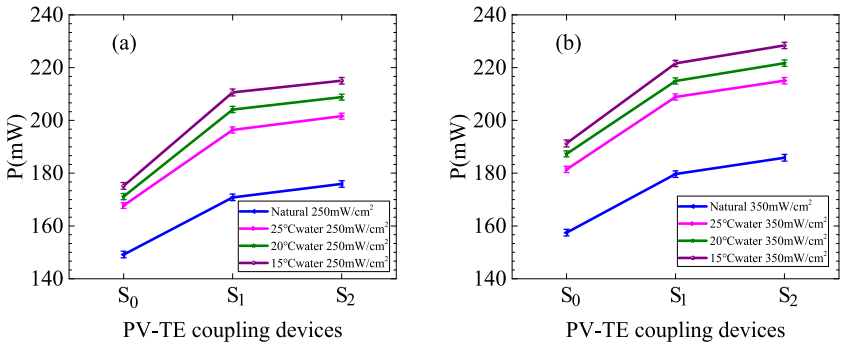

Fig. 6. The total output power (P) of the PV–TE coupling devices varies with the thermal greases with (a) 250 mW/cm^2 and (b) 350 mW/cm^2 radiation and different types of cooling conditions applied.

much more waste heat. The highest increase of TEG performance is 110.6% for the case with coating 4.2 W m^{-1} K^{-1} thermal grease (S_2) when 20 °C water cooling is applied.

Fig. 6 shows that the total output powers (P) have the analogous performances with PV cells (P_{PV}) and TEGs (P_{PV}). The total output power (P) of the PV–TE coupling devices is increased when thermal grease is applied. The total output power (P) of the PV–TE coupling device with 4.2 W m^{-1} K^{-1} thermal grease (S_2) increases by 22.76% when 15 °C water cooling and 250 mW/cm^2 radiation is applied. Results show that using thermal grease can smooth the rough interface, mitigate the negative effects of excessive TCR, and remove the air between the PV cell and the TEG. Coating thermal grease can decrease the TCR between interfaces effectively, and hence enhance the heat transfer from PV cells to TEG accordingly (Qiu et al., 2018, 2019). The thermal conductivity of thermal grease used is the higher, the better. Suitable cooling condition and radiation are also momentous to enhance the PV–TE coupling device performance. Water cooling system can significantly improve the poor heat dissipation which removes the waste heat and maintain the temperature difference of TEG. Cooling system and enhancing solar radiation together can improve the performance of PV cells due to their strongly interaction.

4. Conclusion

In summary, we fabricated the PV–TE coupling device and compared its performance with the pure PV cell under different radiation and cooling conditions. Adopting TEG could minimize the temperature rise of PV cells effectively and enable the wasted heat to generate electricity. Then we try to decrease the thermal contact resistance in PV–TE coupling device by adopting thermal interface materials. The performance of PV–TE coupling devices improve much markedly due to coating thermal interface materials could decrease the thermal contact resistance and enhance heat transfer. The higher thermal conductivity of the thermal grease is, the much better of its effect on optimizing the coupling device performance is. PV–TE coupling device has shown better performance when water cooling is applied in comparison with that when natural cooling is adopted. This work verified the feasibility of using thermal interface materials in PV–TE coupling system, and provided some guidance. Future for this work can reduce thermal contact resistance and enhance the solar radiation to strengthen TEG performance. Moreover, it is worthy to explore different types of PV cell and TEG in PV–TE coupling system. To improve the performance of PV–TE coupling device, more research work needs to be expected further.

Declaration of competing interest

The authors declare that they have no known competing financial interests or personal relationships that could have appeared to influence the work reported in this paper.

CRediT authorship contribution statement

Jia Zhang: Conceptualization, Methodology, Investigation, Writing - original draft. **Han Zhai:** Data curation. **Zihua Wu:** Writing - review & editing. **Yuanyuan Wang:** Visualization, Supervision. **Huaqing Xie:** Project administration, Funding acquisition. **Mengjun Zhang:** Validation.

Acknowledgments

This work was supported by the National Natural Science Foundation of China (51590902 & 51676117 & 51876111) and Graduate Student Foundation of Shanghai Polytechnic University (No. EGD18YJ0018).

References

Baranowski, L.L., Snyder, G.Jeffrey., Toberer, E.S., 2013. Effective thermal conductivity in thermoelectric materials. J. Appl. Phys. 113 (20), 105–114.
Chen, Y., Xuan, Y., 2015. The influence of surface roughness on nanoscale radiative heat flux between two objects. J. Quant. Spectrosc. Radiat. Transfer 158, 52–60.
Deng, Y., Zhu, W., Wang, Y., Shi, Y., 2013. Enhanced performance of solar-driven photovoltaic-thermoelectric hybrid system in an integrated design. Sol. Energy 88, 182–191.
Dubey, S., Sarvaiya, J.N., Seshadri, B., 2013. Temperature dependent photovoltaic (PV) efficiency and its effect on PV production in the world-a review. Energy Procedia 33 (33), 311–321.
Grujicic, M., Zhao, C.L., Dusel, E.C., 2005. The effect of thermal contact resistance on heat management in the electronic packaging. Appl. Surf. Sci. 246 (1), 290–302.
He, W., Zhang, G., Zhang, X., et al., 2015. Recent development and application of thermoelectric generator and cooler. Appl. Energy 143, 1–25.
Huen, P., Daoud, W.A., 2016. Advances in hybrid solar photovoltaic and thermoelectric generators. Renew. Sustain. Energy Rev. 72, 1295–1302.
Liao, T., Lin, B., Yang, Z., 2014. Performance characteristics of a low concentrated photovoltaic– thermoelectric hybrid power generation device. Int. J. Therm. Sci. 77, 158–164.
Liu, C., Chang, M., Chuang, C., 2014. Effect of rapid thermal oxidation on structure and photoelectronic properties of silicon oxide in monocrystalline silicon solar cells. Current Appl. Phys. 14 (5), 653–658.
Ma, W.G., Miao, T.T., Zhang, X., et al., 2015. Comprehensive study of thermal transport and coherent acoustic-phonon wave propagation in thin metal film–substrate by applying picosecond laser pump-probe method. J. Phys. Chem. C 119 (9), 5152–5159.
Meneses-RodríGuez, D., Horley, P.P., González-Hernández, J., et al., 2005. Photovoltaic solar cells performance at elevated temperatures. Sol. Energy 78 (2), 243–250.
Mirmira, S., Marotta, E., Fletcher, L., 1997. Thermal contact conductance of adhesives for microelectronic systems. J. Thermophys. Heat Transfer 11 (2), 141–145.
Pang, W., Liu, Y., Shao, S., Gao, X., 2015. Empirical study on thermal performance through separating impacts from a hybrid PV/TE system design integrating heat sink. Int. Commun. Heat Mass Transfer 60, 9–12.
Prasher, Ravi S., 2001. Surface chemistry and characteristics based model for the thermal contact resistance of fluidic interstitial thermal interface materials. J. Heat Transfer 123, 969–975.

Qiu, L., Guo, P., Kong, Q., et al., 2019. Coating-boosted interfacial thermal transport for carbon nanotube array nano-thermal interface materials. Carbon (145), 725–733.
Qiu, L., Guo, P., Zou, H., et al., 2018. Extremely low thermal conductivity of graphene nanoplatelets using nanoparticle decoration. ES Energy & Environment 2, 66–72.
Qiu, L., Scheider, K., Radwan, S.A., et al., 2017. Thermal transport barrier in carbon nanotube array nano-thermal interface materials. Carbon 120, 128–136.
Qiu, L., Zou, H., Wang, X., et al., 2018. Au nanoparticle-boosted interfacial interaction enhances the electrical and thermal conductivities of carbon nanotube fibers. Carbon.
Radziemska, E., 2003. The effect of temperature on the power drop in crystalline silicon solar cells. Renew. Energy 28 (1), 1–12.
Sarvar, F., Whalley, D., Conway, P., 2006. Thermal interface materials - a review of the etate of the art. In: IEEE 2006 1st Electronic System Integration Technology Conference.
Skoplaki, E., Palyvos, J.A., 2009. On the temperature dependence of photovoltaic module electrical performance: A review of efficiency/power correlations. Sol. Energy 83 (5), 614–624.
Thirugnanasambandam, M., Iniyan, S., Goic, R., 2010. A review of solar thermal technologies. Renew. Sustain. Energy Rev. 14 (1), 312–322.
TrittT, M., Böttner, H., Chen, L.D., 2008. Thermoelectrics: direct solar thermal energy conversion. MRS Bull. 33, 366–368.
Tyagi, V.V., Rahim, N.A.A., Rahim, N.A., et al., 2013. Progress in solar PV technology: Research and achievement. Renew. Sustain. Energy Rev. 20 (4), 443–461.
Venkatasubramanian, R., Silvola, E., Colpitts, T., O'Quinn, B., 2001. Thin-film thermoelectric devices with high room-temperature figures of merit. Nature 413, 597–602.
Vorobiev, Y., González-Hernández, J., Vorobiev, P., et al., 2006. Thermal-photovoltaic solar hybrid system for efficient solar energy conversion. Sol. Energy 80 (2), 170–176.
Wu, Y.Y., Wu, S.Y., Xiao, L., 2015. Performance analysis of photovoltaic–thermoelectric hybrid system with and without glass cover. Energy Convers. Manag. 93, 151–159.
Wysocki, J.J., Rappaport, P., 1960. Effect of temperature on photovoltaic solar energy conversion. J. Appl. Phys. 31 (3), 571–578.
Yin, E., Li, Q., Xuan, Y., 2017. Thermal resistance analysis and optimization of photovoltaic-thermoelectric hybrid system. Energy Convers. Manag. 143, 188–202.
Zhang, Q., Ai, X., Wang, L., et al., 2015. Improved thermoelectric performance of silver nanoparticles-dispersed Bi_2Te_3 composites deriving from hierarchical two-phased heterostructure. Adv. Funct. Mater. 25 (6), 966–976.
Zhang, J., Xuan, Y., Yang, L., 2014. Performance estimation of photovoltaic-thermoelectric hybrid systems. Energy 78, 895–903.